

Controlled Nucleation of Metal Sulfide Layers via Surface Functionalisation with Sulfur Species: Enhanced Initial Growth of GaS_x Thin Films

Zsófia Baji, Zoltán Kovács, Zoltán Szabó, Orsolya Hakkal, Attila Sulyok, Zsolt Fogarassy, Zsófia Bérces, János Volk
HUN-REN Centre For Energy Research
1121. 29-33. Konkoly-Thege Miklos str. Budapest, Hungary

Abstract

The initial stages of the atomic layer deposition (ALD) of metal sulfide thin films are hindered by delayed nucleation and poor film continuity. The present work explores the nucleation of gallium sulfide (GaS_x) films using hexakis(dimethylamino)digallium and H₂S as precursors. Smooth amorphous GaS_x layers were deposited, with their composition confirmed by XPS and their structure examined by TEM. Post-deposition annealing in H₂S was attempted to induce crystallinity. To address the nucleation barrier, a novel surface functionalization strategy was developed: replacing surface hydroxyl groups with sulfur containing species prior to deposition. Different functionalisation treatments were tested, which significantly enhanced nucleation, as demonstrated by accelerated initial growth and improved film uniformity even at low cycle numbers. These results establish chemically specific surface functionalization as an effective strategy to promote a controlled nucleation of sulfide thin films.

I. Introduction

Atomic layer deposition is a chemical thin film deposition method which utilizes the consecutive chemisorption of precursor materials separated by purges by an inert gas [1,2]. The reactants only form the composite layer on the substrate surface. The method provides several key benefits, such as excellent conformity, and a precise control of composition and thickness, even at low temperatures [3,4].

Metal chalcogenide thin films, particularly transition metal sulfides and selenides, currently attract an intense research effort due to their exceptional mechanical, optical, electrical and magnetic properties and their promise in a number of applications in electronics [5], optoelectronics[6], catalysis [7], and

energy storage [8]. Transition metal dichalcogenides (TMDCs) are layered materials such as MoS₂ or WS₂ [9], which are especially interesting as they are 2D materials held together by weak Van der Waals forces. They are promising candidates for next-generation transistors, photodetectors, and catalysts for reactions such as the hydrogen evolution reaction (HER [10]). Their performance often depends critically on film thickness, as one or two layers of the material may show very different electron structure from the bulk counterpart, including ferromagnetism in single layers [11]. Their continuity, crystallinity, and uniformity are all influenced by the initial stages of layer growth [12, 13].

While TMDCs have been extensively studied for their semiconducting and optoelectronic properties, other metal sulfides, and especially transition-metal monosulfides remain relatively underexplored. Even if their direct electronic applications are more limited than those of TMDCs, their comparatively simple stoichiometry and unique bonding environments present promising opportunities in applications, such as catalysis (e.g., hydrogen evolution reaction) due to their surface chemistry, as well as in non-volatile memory storage devices owing to their resistive switching behaviour [14]. In particular, gallium sulfide (GaS_x) is a wide band gap semiconductor with two stable allotropes: GaS and Ga₂S₃. Gallium-sulfides have been deposited by PVD [15], CVD [16] and ALD [17-21], which offers a better control over stoichiometry conformity and thickness.

The atomic layer deposition of GaS_x layers has been reported previously with the use of different precursors, such as hexakis(dimethylamino)digallium (Ga(NMe₂)₃)₂ yielding amorphous GaS layers [17,18], and trimethylgallium, which resulted in amorphous Ga₂S₃ films [19]. These precursors were combined with H₂S. The use of H₂S plasma makes growth temperatures as low as 70°C, and the growth of crystalline Ga₂S₃ layers possible [20]. The chemistry of these processes has been further investigated in mechanistic studies [21].

The control of the nucleation of ALD growth is crucial for the research of ultrathin or 2D layers, the preparation of functional nanoparticles and area selective atomic layer deposition. However, most reports on sulfide ALD focus on the deposition parameters and film properties, while surface-chemistry strategies for enhancing sulfide nucleation remain largely unexplored. The atomic layer deposition (ALD) and atomic layer annealing/deposition methods of sulfide films face significant nucleation difficulties, especially on oxide substrates such as SiO₂. The standard hydroxyl (-OH) surface

termination common to oxide substrates is not an ideal anchoring site for metal sulfide growth. According to Zhao and Wang, the agglomeration of the sulfide material (NiS) can be expected in the first few ALD cycles [22], which leads to delayed nucleation, and island-like growth.

A crucial hindering factor in ALD nucleation is the number of reactive sites on the surface. In the case of Si substrates, ALD growth starts by the chemisorption of the precursor molecule to the surface -OH species. However, about the hydroxyl coverage of SiO_x surfaces, there is only the often cited research of Haukka et al. [23] who examined precursor adsorption on thermal, CVD and porous silica surfaces, and found about 1–7 active sites on every nm² of the SiO₂ surface. Of course, SiO₂ has different types of active surface sites, including single hydroxyls, vicinal pairs, or geminal groups, as well as different active surface oxygen binding sites, all of which have different affinities regarding certain precursors. Therefore, there are no conclusive measurement data on surface hydroxyl coverage, especially on native SiO₂, which is the most common substrate in ALD research.

The nucleation of ALD layers is also hindered by reaction kinetics, thus longer precursor exposures in the first growth cycle help the adsorption of precursor molecules to all available reaction sites in the initial phase of the growth [24, 25]. A chemical pretreatment of the substrate surface is an often-used method that increases the density of the chemically active groups, that is, the hydroxylation of the surface. This may involve an acidic pretreatment, or a plasma or UV activation followed by dipping the sample in water to fill the broken bonds with hydroxyl groups.

Oxygen plasma and UV-based treatments are widespread methods to clean and activate oxide surfaces, removing impurities, generating reactive sites by breaking Si–O–Si bonds, and generating highly reactive, under-coordinated surface sites. These processes can partially dehydroxylate and chemically activate the surface. Stable hydroxyl termination is therefore only achieved after subsequent exposure to water, either intentionally or via ambient humidity. In fact, oxygen plasma-treated substrates transferred directly to the ALD reactor exhibited poorer GaS_x nucleation than untreated surfaces, indicating that surface activation alone is insufficient without controlled hydroxylation. By contrast, wet chemical oxidation using piranha solution produced a well-defined hydroxylated surface and enabled more reproducible and enhanced nucleation than plasma treatment [25].

The growth rate in steady ALD growth can be described as a function of the precursor size and the distances of the available binding sites on the surface [26]. The nucleation is even more complex, and several different mathematical models were used to reliably describe it [27-30]. Puurunen et al. [29,30] described ALD nucleation as an island-growth process, where the islands expand and eventually coalesce depending on the surface chemistry and precursor properties. They also developed a mathematical description linking growth-per-cycle behaviour to these fundamental physical and chemical parameters.

In the present work, a novel approach for the surface functionalisation of the substrate for sulfide layer deposition was explored: the functionalization of the surface with sulfur-containing species to promote the nucleation of sulfide films. The motivation is that sulfide layers bond more favourably to -S-R surface groups (where R can be H, CH₃, etc.) compared -OH groups, thus preventing the re-nucleation that occurs in each cycle on hydroxylated surfaces. In addition, different silicon oxide surfaces were compared with respect to their influence on nucleation.

To the best of the authors' knowledge, this approach—specifically the conversion of -OH groups to sulphur containing surface species on silicon for enhancing sulfide ALD nucleation—has not been previously reported. While organosulfur and disulfide precursors (e.g. DMDS, DTBDS) have been used as sulfur sources in metal-sulfide ALD, a systematic demonstration that gas-phase disulfide surface functionalisation can enhance sulfide nucleation on oxidised silicon has not been reported. Although surface thiolation methods exist in the literature, they are most often applied to metallic substrates such as gold, where Au-S bonds readily form. This strategy is demonstrated using gallium sulfide (GaS_x) as a model system. By preparing thiol or alkylthio terminated silicon surfaces and performing ALD-like depositions with hexakis(dimethylamino)digallium and H₂S, a significantly enhanced initial growth and nucleation density can be seen.

II. Experimental

The sulfide films were prepared in a Picosun R-200 ALD reactor. Ultra-high purity nitrogen (6N, Messer) was used as both the carrier and purging gas. The gallium precursor was

hexakis(dimethylamino)digallium $\text{Ga}_2(\text{NMe}_2)_6$ 98%, (Strem Chemicals), and the sulfur source was a premixed gas of 10% H_2S in Ar. $\text{Ga}_2(\text{NMe}_2)_6$ was selected in part to avoid the introduction of oxygen-containing ligands, as oxygen incorporation is undesirable for the growth of gallium sulfide films. Compared to alkyl gallium precursors such as GaMe_3 , it does not contain direct Ga–C bonds, while in contrast to β -diketonate precursors (e.g., $\text{Ga}(\text{acac})_3$ or $\text{Ga}(\text{thd})_3$), it exhibits sufficient reactivity toward sulfur-containing co-reactants at moderate temperatures. Depositions were carried out at 200 °C, resulting in smooth and amorphous layers. This temperature is within the ALD window according to ref.18, and it is confirmed by the present experimental work. The Ga-precursor was pulsed from a picohot booster source and was heated to 135°C to achieve sufficient vapour pressure, and a 1.1 s fill time and 0.5 s pulse time were applied. With this, the pulse lengths during deposition were 0.1s followed by a 4 s purging in the case of the H_2S pulse and 1.5 s dosing of the $\text{Ga}_2(\text{NMe}_2)_6$ precursor followed by a 4 s purge. For the continuous layer deposition, 1000 cycles were applied. To induce crystallization, the as-deposited films were annealed in the same reactor at 420 °C. Annealing was performed by pulsing H_2S gas in a flow-stop mode, where each gas pulse was followed by closing the reactor to allow a dwell period before the next pulse. The pulse lengths were 0.3 s, and the flow stop steps were 220s.

Nucleation experiments were conducted by depositing GaS_x films with varying cycle numbers: 3, 5, 10, 15, 20, and, in cases of particularly slow nucleation, 25 cycles.

To assess the influence of oxide type on nucleation behaviour, the nucleation on untreated native oxide-covered Si, 100 nm thermal oxide-covered Si, and 100 nm CVD oxide-covered Si was compared. To examine the effect and surface chemistry, chemically modified silicon surfaces were investigated: piranha-pretreated native oxide-covered Si (15 min in $\text{H}_2\text{SO}_4:\text{H}_2\text{O}_2 = 4:1$) to enhance hydroxyl coverage, native oxide-covered Si pretreated with a long dimethyl disulfide (DMDS) pulse, native oxide-covered Si pretreated with a long di-tert-butyl disulfide

(DTBDS) pulse, piranha-pretreated Si followed by a long DTBDS pulse, and thiolated thermal oxide surfaces. In the case of DMDS or DTBDS pulses, the samples were mounted into the ALD reactor and exposed to a 10 s pulse of dimethyl disulfide or di-tert-butyl disulfide prior to deposition. The thiolated surfaces were prepared by placing previously hydrophilized Si substrates in mercaptopropyl-trimethoxysilane vapour in a nitrogen atmosphere for 12 hours. The three different surface functionalization approaches are shown in fig.1.

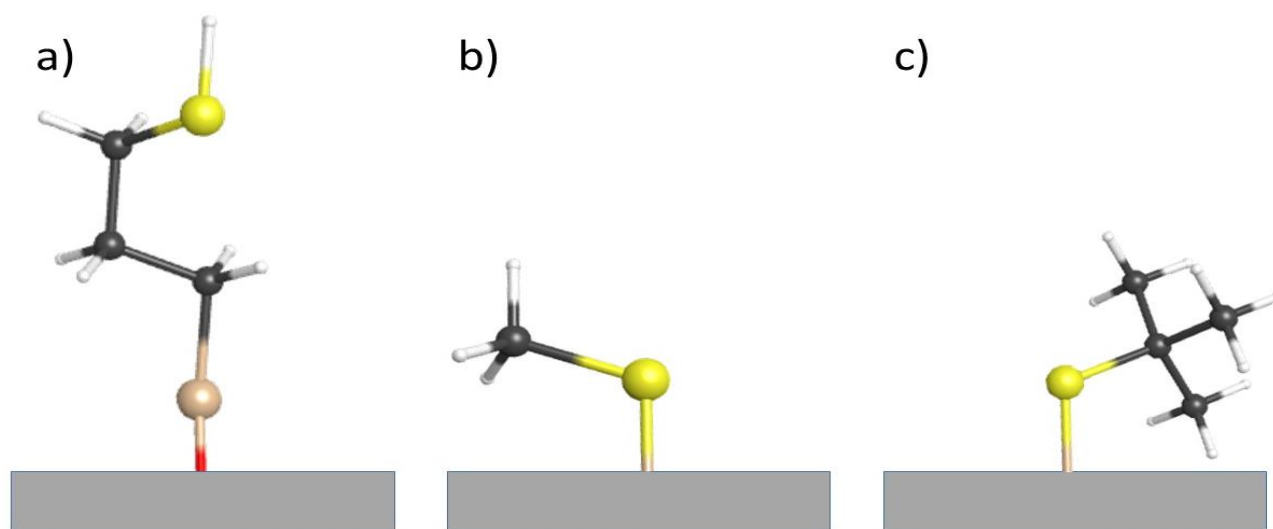


Fig.1. Schematic illustration of the three surface functionalisation approaches applied to silicon oxide substrates prior to GaS_x deposition. a) silane-based thiolation using mercaptopropyl-trimethoxysilane, yielding an organic spacer layer terminated with –SH groups; b) gas-phase treatment with DMDS c) or DTBDS producing sulphur-containing surface species The grey line represents the native Si-oxide surface covered by surface hydroxyl groups. The yellow balls mean sulfur, black carbon, white hydrogen and brown silicon atom.

Elemental composition including the separation of different chemical bonds was determined by XPS measurements at and below the surface. The XPS spectra were detected by Escalab Xi+ (produced by Thermo Fisher) equipment with 0.6 eV energy resolution using monochromatized

Al K α source with 0.65 mm spot. While surface layers may contain contamination and oxidation, the internal composition was probed by sequentially removing the upper layers using Ar ion sputtering. A large enough and evenly sputtered area was achieved using a 500 eV Ar⁺ beam rastered to 2.5 mm. The photoemission peaks were collected around the Ga 2p 3/2 (1122 eV), S 2p (162eV), O 1s (532 eV), and C 1s (284 eV) core levels. Decomposition of complex peak shapes was carried out with a peak fitting algorithm using the built-in Avantage software of Escalab equipment. Peak intensity was quantified by the area of the peak and the composition was calculated by assuming a homogeneous target with the built-in sensitivity factor. Elemental concentrations were calculated excluding oxygen species associated with carbon contamination. This exclusion is justified because Ga-related oxygen is well separated from oxygen bound to C and Si, and the latter is less relevant to the film composition.

The nucleated layers were examined with an AIST-NT, SmartSPM atomic force microscope (AFM) in tapping mode. AFM data were processed as follows. Raw height maps were plane-corrected and line-wise flattened to remove the scanner bow. A conservative absolute threshold for island detection was defined as the mean baseline height of a bare substrate scan plus twice the baseline noise (RMS roughness). Coverage was computed as the fraction of pixels exceeding this threshold. For each sample, three independent 0.5 \times 0.5 μ m scans were analysed. The most relevant samples were also investigated by high-resolution transmission electron microscopy (TEM) with a Titan Themis 200 image corrected TEM/STEM microscope. For the energy dispersive spectrometry (EDS), a Super-X detector was used. The cross-sectional samples were prepared by focused ion beam.

III. Results and discussion

A. Film growth



This is the author's peer reviewed, accepted manuscript. However, the online version of record will be different from this version once it has been copyedited and typeset.
PLEASE CITE THIS ARTICLE AS DOI: 10.1116/6.0005254

ALD GaS layers were deposited using $\text{Ga}_2(\text{NMe}_2)_6$ and H_2S . The deposition temperature of 200°C and the precursor parameters were based on those reported in ref.18. The growth rate was $0.5 \text{ \AA}/\text{cycle}$ (from the thickness determined from the TEM measurements), and the deposited layers were uniform. To improve the layer quality, post deposition annealing procedures were carried out in the same ALD reactor, at 420°C . A sulfur-containing atmosphere was provided by pulsing H_2S into the nitrogen flow of the reactor.

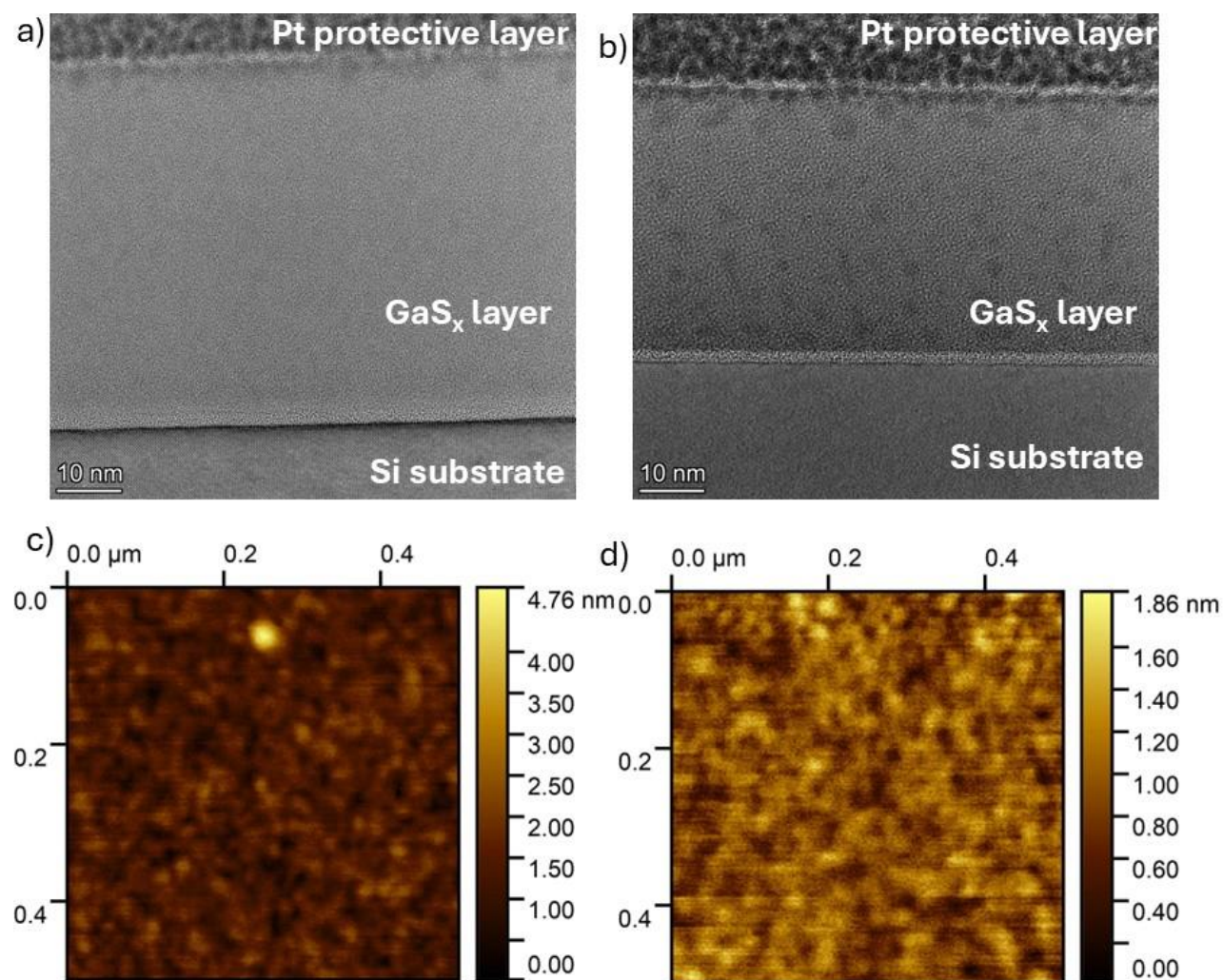


Fig 2. The TEM micrographs of the cross section of the film: a) the as deposited, and b) the annealed layer. The morphology of the layers, as measured with AFM: c) the as deposited surface, d) the annealed one

Fig 2a shows that the as-deposited film was indeed amorphous, which is consistent with the relatively low deposition temperature. After annealing the layers at 420 °C for 5 hours (Fig.2b), some crystallisation began, but still only few nm sized crystallites formed randomly in the layer, with a higher amount of them at the surface of the film. The absence of long-range order even after a heat treatment suggests that the crystallization of GaS_x requires a higher temperature or higher sulfur content in the annealing atmosphere. AFM measurements (fig.2c and d) showed that the deposited layers were very smooth, with an RMS roughness of 0.4 nm. The morphology of the annealed layer did not roughen either, which is consistent with fig. 12b, and the fact that the crystallisation was not complete even after a 5h annealing.

XPS measurements were used to determine the in-depth composition of the GaS films. Depth profile with Ar sputtering was detected until a stable concentration plateau was reached. The removed thickness is ~1nm/cycle based on Ta₂O₅ erosion rate. Some details are shown in Fig 3. Fig 3a shows a spectrum detected at the internal part of the as-deposited GaS layer. The Ga 2p peak shows a single state corresponding to Ga-sulfide state. The sulfur 2p peak is loaded with the coinciding Ga 3s peak but the decomposition reveals their own intensity separately. Besides the visible sulfide state, no other state with higher oxidation degree was detected. Carbon 1s peak is minor and smeared thus not interpreted. The O1s peak is a composition of oxygen in Ga-oxide and oxygen in C-O or Si-O bond. Calculated composition is shown in Fig 3b for the as deposited and Fig 3c for the annealed layer. Indicated a gallium-to-sulfur ratio consistent with gallium monosulfide (GaS) and a uniform composition throughout the analysed depth, suggesting homogeneous film growth. No significant oxygen signal was detected on the surface, confirming that the layers were not oxidised after exposure to air. This implies that the deposited GaS material exhibits good chemical stability under ambient conditions.

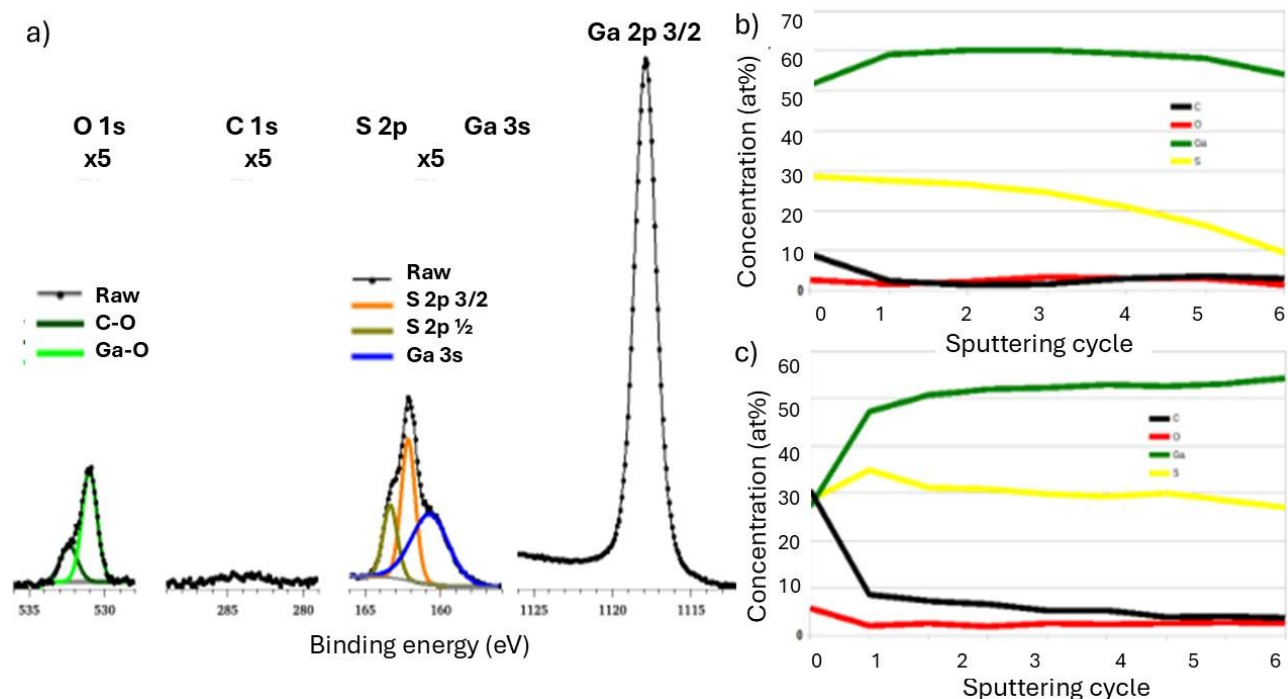


Fig.3. XPS characterisation of GaS layers: a) Photoemission spectra acquired around the O 1s, C 1s, S 2p/Ga 3s, and Ga 2p_{3/2} core levels from the as-deposited GaS surface; elemental concentration profiles as a function of sputtering time (or sputtering cycles) for b) the as-deposited layer and c) the annealed layer, calculated from XPS depth-profile measurements.

The as-deposited GaS layers were optically completely transparent and colourless, appearing practically invisible on the substrate surface. This observation was confirmed by the optical transmittance measurements, which (after subtraction of the bare substrate contribution) showed values of approximately 80% at shorter wavelengths, increasing to about 90% at longer wavelengths in the visible–near-infrared range. The optical band gap was estimated from a Tauc-plot (see inset), assuming a direct allowed transition, yielding a value of approximately 4 eV. This optical gap is in accordance with earlier published data for crystalline GaS (3-3.5 eV), but is somewhat wider, due to the amorphous nature or low crystallinity of the films. The extracted value should therefore be regarded as an effective optical gap characteristic of the amorphous GaS_x films grown under these conditions.

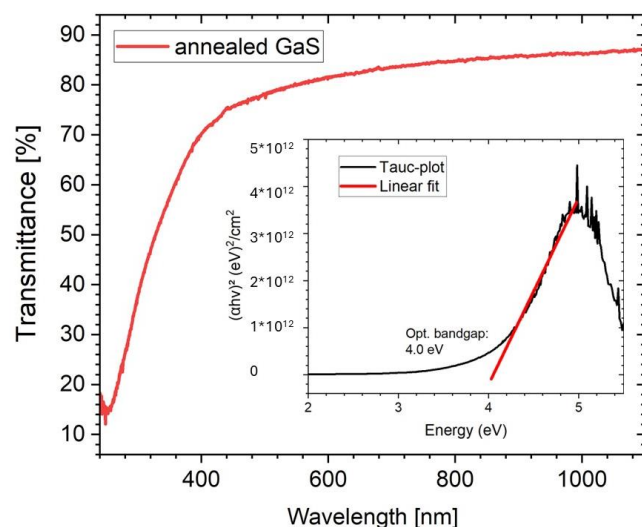


Fig.4. Transmittance measurement and the Tauc-plot of the above 500 nm thick GaS layer deposited at 200°C, annealed at 420°C

B. Nucleation of GaS films

The main purpose of this study was to investigate the nucleation behaviour of sulfide materials, through the example of GaS, on silicon substrates, and to explore how surface modifications, such as increasing hydroxyl coverage or introducing surface-bound sulfur containing groups, affect the initial stages of growth. The density, size, and distribution of chemically active anchoring sites on the surface govern the nucleation process. Therefore, studying these factors provides fundamental insights into the mechanisms controlling sulfide nucleation, as well as possible methods to enhance these processes.

The first question to address was how the type of silicon oxide influences nucleation. To investigate this, thermal, CVD-grown, and native oxide-covered silicon surfaces were compared. Fig.5. shows the AFM micrographs of the pristine surfaces (a-c) and the surfaces after 15 cycles. As CVD and thermal oxide surfaces were quite rough, the nucleated islands cannot be discerned directly, and a quantitative analysis of coverage is not possible. Nevertheless, after 15 cycles of ALD, subtle differences can be found. XPS measurements

confirmed that thermal oxide exhibited a 30% higher nucleation density than native oxide, and CVD oxide had a 90% higher surface coverage, suggesting that the chemical and structural characteristics of the oxide layer play a significant role. Despite this, native oxide remains the standard choice for ALD growth, and also offers a reproducible surface for growth studies.

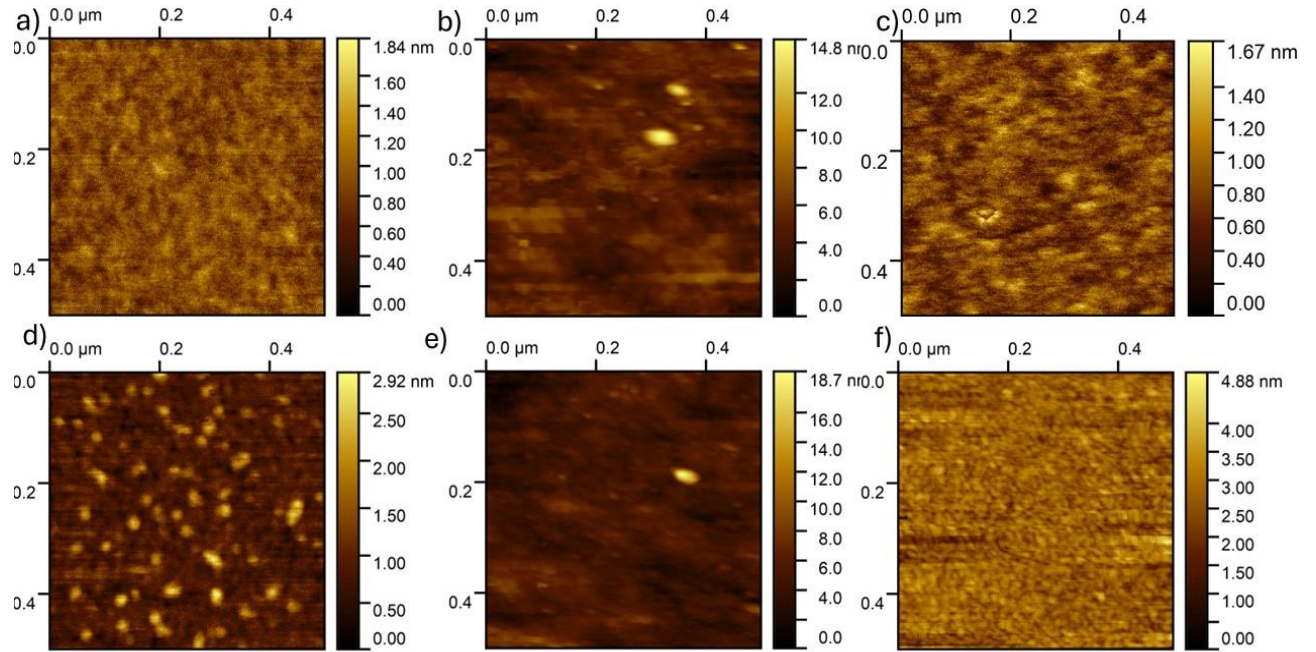


Fig.5. The surfaces of the different oxides: a) native Si-oxide, b) CVD oxide and c) thermal oxide; and their morphologies after 15 deposition cycles: d) deposition on native oxide, e) deposition on CVD oxide, and f) deposition on thermal oxide.

The nucleation behaviour of GaS layers was systematically examined by depositing 3, 5, 10, 15, 20, and 25 ALD cycles. The AFM images clearly demonstrate that GaS growth on native SiO₂-terminated silicon proceeds in an island-like manner, consistent with a Volmer–Weber growth mode. This behaviour is attributed to the limited density of reactive surface sites that can chemically bond with the metal precursor during the initial cycles. On SiO₂ surfaces, surface hydroxyl groups are the primary reactive sites for precursor chemisorption, although other oxygen-containing sites (for example bridging or non-bridging oxygens associated with

defects) can also participate. To promote a higher nucleation density, various surface pretreatments were explored with the goal of increasing the number or reactivity of such sites. The AFM images of GaS after five ALD cycles on differently pretreated Si substrates (Figure 6) reveal pronounced effects of surface chemistry on nucleation behaviour. All samples have some nucleated material on the surface after 5 cycles across all of the scanned area, but the surface coverage and morphology change with pretreatment. On native SiO₂ (Figure 6a), the low density of islands visible indicates sparse nucleation, pointing towards a low density of reactive sites for Ga precursor chemisorption. The piranha-treated surface (Figure 6b), enriched in hydroxyl groups, shows a higher density of islands, a broader distribution of island sizes pointing towards partial coalescence, which is consistent with enhanced precursor adsorption. Increasing the -OH coverage of the surface has previously proven effective in promoting nucleation for oxide-type ALD processes. Piranha treatment was employed for this purpose, as it efficiently hydroxylates the surface. However, an agglomeration of sulfide materials on hydroxylated surfaces often arises because the cohesive interactions within the sulfide layer are stronger than its adhesion to the underlying -OH-terminated substrate. As a result, rather than forming a uniform film, the material tends to cluster into islands. In subsequent ALD cycles, new growth must nucleate on the exposed substrate between these islands, slowing film coalescence and producing a rough, discontinuous morphology.

To solve this issue, an alternative chemical strategy is proposed: converting surface hydroxyl groups into sulfur containing surface species. According to the available literature, the direct substitution of surface hydroxyl groups with terminal -SH groups on SiO₂ is not feasible under practical conditions, because Si-S-H terminations are intrinsically unstable. The Si-S bond oxidises or hydrolyses in the presence of trace moisture, and the -SH group itself is not sufficiently nucleophilic to displace surface -OH groups. Consequently, established “thiolation” procedures for oxidised silicon do not form Si-SH terminations. Instead, they rely

on silane coupling agents such as mercaptopropyl-trimethoxysilane, which anchor to the substrate via Si–O–Si linkages while presenting a terminal $-(\text{CH}_2)_3\text{-SH}$ group [31.]. This treatment therefore produces an organic spacer layer between the inorganic substrate and the sulphur functionality, rather than a direct sulphur termination of the oxide surface. While such layers introduce accessible sulphur groups, the presence of the alkyl chain modifies both steric environment and surface energetics relative to a hypothetical Si–SH termination.

This approach was performed by placing the substrates in a sealed environment in N_2 atmosphere with mercaptan vapour at room temperature for 12 hours. Previously, the substrates were thoroughly cleaned, and their -OH coverage was increased by a piranha treatment. This way a high -OH coverage could be exchanged into -O-Si-R-SH species. However, the process also significantly roughened the substrate, complicating AFM interpretation and possibly introducing unwanted surface inhomogeneity. Despite this, XPS measurements confirmed the presence of adsorbed thiol molecules on the surface, indicating that chemical exchange between -OH and -SH containing groups had indeed occurred, even if the resulting surface morphology was suboptimal.

To achieve a cleaner and more controlled surface sulfidation, a novel gas-phase approach was developed using dimethyl disulfide (DMDS) [32], which is known as an organosulfur precursor in atomic layer deposition, as an alternative to H_2S , as well as di-tert-butyl disulfide (DTBDS) [33]. The underlying process is assumed to be a dissociative chemisorption of dialkyl disulfides with the cleavage of the S–S bond to yield surface-bound alkylthiolate intermediates (e.g. $\text{CH}_3\text{S-}$), which can serve as reactive sulphur donors in subsequent metal-sulphide formation, although the adsorption mode is also substrate dependent. Consequently, disulfide exposure may be a plausible route to increase surface sulphur content and to promote ALD sulfidation, even though the exact nature of the surface species (thiolate, alkylthio, physisorbed disulfide, H-bonded complex) is yet uncertain [32-34]. According to the proposed mechanism in ref. 32.,

the most likely interaction between DMDS and the surface involves the breaking of the S–S bond, producing two methyl-sulphur fragments that subsequently bond to the substrate. This process creates two sulfur bound methyl groups on the surface, which remain chemically reactive towards the metallic precursor, or subsequently, these methyl groups may even leave the surface leaving an active surface thiol group behind via an intramolecular β -H transfer process, liberating a gaseous isobutene molecule. Thus, theory suggests that this surface modification may facilitate more stable sulfide bonding during the initial ALD cycles.

The treatment was performed directly in the ALD reactor under standard operating conditions, allowing precise control of temperature and exposure. Replacing surface –OH groups with sulphur-containing species using dimethyl disulfide (Fig.6c) further increased nucleation density, producing a fine distribution of small islands. The roughness scale is slightly lower on this image, but the coverage is much higher than 6a or 6b. This implies that this approach provides a high nucleation site density and faster approach to coalescence. This treatment yielded a more favourable anchoring chemistry for sulfide nucleation than -OH, leading to a nearly continuous film coverage after only 15–20 ALD cycles. This strongly suggests that DMDS effectively modifies the surface chemistry by introducing reactive sulfur species, which act as nucleation sites for subsequent GaS growth.

Di-tert-butyl disulfide (DTBDS) was tested as an alternative sulfur-donating agent, as it is also used in some metal-sulfide ALD processes. Although DTBDS had shown limited reactivity in our previous ALD experiments, its use here led to a measurable improvement in nucleation compared to the untreated substrates. The di-tert-butyl disulfide-treated sample (Fig.6.d) exhibits a similar but slightly less dense pattern with coarser, somewhat larger but less dense islands, likely due to steric hindrance of the bulky tert-butyl ligands, limiting effective exposure. This suggests that disulfide-based precursors in general may play a beneficial role in surface

activation for sulfide film growth, even if their efficiency varies depending on molecular structure and surface affinity.

Building upon these results, a two-step surface pretreatment sequence was tested to further enhance the nucleation process. First, the substrates were treated with piranha solution to increase the density of surface hydroxyl groups. Immediately following this, the samples were placed into the reactor and subjected to a long DMDS pulse to convert these hydroxyls to S-bound species, through an in-situ gas-phase exchange reaction. This combined treatment indeed yielded the best results, producing a higher surface coverage after 5 cycles, as shown in fig. 6.c. The nucleation of this film was more uniform with fine, closely packed features with minimal uncovered areas. This shows that an initial hydroxylation followed by efficient exchange of -OH groups to $-S(CH_3)_3$ provides an optimal surface for Ga precursor adsorption and GaS nucleation. The thiolated surface (Fig.6.f) also shows a higher degree of coverage, but also an increased surface roughness. This procedure resulted in a continuous coverage even after 15 cycles. The RMS roughness of these films was also significantly lower than that of the untreated or mercaptan-treated samples, confirming that the nucleation process was more uniform and the film growth more consistent.

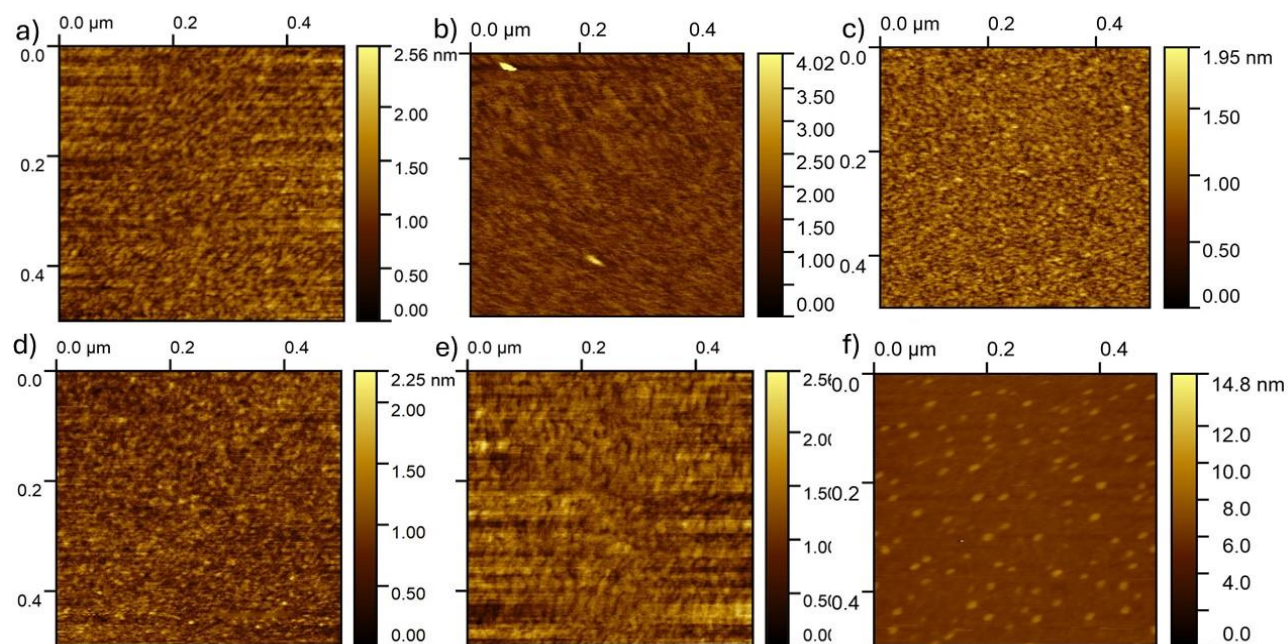


Fig.6. AFM micrographs of a) 5 cycles of GaSx on native oxide covered Si, b) the same with piranha pretreatment, c) DMDS pretreatment, d) di-tert-butyl-disulfide pretreatment, e) piranha+DMDS pretreatment, and f) thiolation with mercaptopropyl-trimethoxysilane

The same trends were visible after more deposition cycles as well, thus, surface functionalisation with sulphur-containing species was found to have a definite influence on GaS nucleation behaviour. The introduction of chemically compatible bonding sites significantly increased the density of nucleation centres, leading to more uniform and continuous films after only a few deposition cycles. In contrast, surface treatments that produced bulky ligands appeared to lower the effective density of accessible sites, resulting in larger, more isolated islands. Hydroxylation alone improved nucleation relative to the untreated substrate, however, direct sulphur functionalisation produced far superior results, indicating that the effectiveness of nucleation depends on the chemical nature of the surface termination as well as its density. Several mechanisms may account for this behaviour. Chemical matching between the sulphur-terminated surface and the sulphide layer being deposited likely plays a key role. Sulphur-containing surface groups are chemically similar to the sulphide anions in GaS, making them

more compatible with the ligands and reaction pathways of the gallium precursor. This favours chemisorption and ligand-exchange reactions during the earliest stages of deposition, facilitating the formation of the first GaS bonds and promoting rapid sulfidation of the surface. Sulfur-containing surface species are also more reactive than hydroxyl groups in part because sulfur is less electronegative and more polarizable than oxygen, making its lone pairs more available for bonding. On the other hand, S-H bonds are less polar and are bonded to hydrogen weaker than O-H bonds, which reduces steric and electrostatic hindrance at the surface. Together, these properties increase the nucleophilicity and reactivity of the sulfur atoms, making them more effective at interacting with gallium precursors during the initial stages of nucleation.

Steric hindrance also influences the efficiency of nucleation. The molecular structure of the modifying agent determines both the distribution and the accessibility of reactive surface groups. Short, simple sulphides such as DMDS can yield a compact and accessible sulphur coverage, whereas bulkier molecules such as DTBDS may form loosely packed or sterically hindered layers, limiting the number of active sites available for precursor adsorption.

A further consideration is the interplay between site density and island morphology. When the density of reactive surface sites is high, numerous small nuclei are formed, which rapidly coalesce into continuous films. Conversely, when the site density is low, fewer but larger islands develop, extending the incubation period before complete coverage. Thus, an optimal surface modification should maximise the density of chemically compatible, spatially accessible sulphur species without introducing excessive steric hindrance.

After 20 ALD cycles, the samples were further characterised using XPS, as an independent validation of the AFM analysis. Because the deposited films formed discrete islands rather than continuous layers, it was not possible to obtain precise quantitative measurements of surface coverage. To overcome this limitation, the relative amount of gallium present on the silicon

This is the author's peer reviewed, accepted manuscript. However, the online version of record will be different from this version once it has been copyedited and typeset.
PLEASE CITE THIS ARTICLE AS DOI: 10.1116/1.5005254

surface was measured for each sample. The measurement on untreated Si was used as a reference, and the results from all other samples were compared relative to this baseline. The estimated surface coverage of GaS_x was found to increase with the surface functionalization. Relative to native SiO₂, DMDS treatment increased the estimated coverage by approximately 2.6×, combined piranha + DMDS treatment by 2.6×, and thiolated thermal oxide by 2.4×. Although absolute coverage values are approximate due to uncertainties in island thickness and shape, these relative increases clearly demonstrate the effectiveness of sulfur-containing surface treatments in promoting nucleation. Surface coverage values obtained from AFM images were thus compared with the relative gallium amounts determined by XPS. In cases where discrepancies were observed, the AFM-derived values were reassessed and adjusted to ensure consistency with the XPS data. Thus, the surface coverage values were derived from the AFM images, which were calibrated with the XPS results.

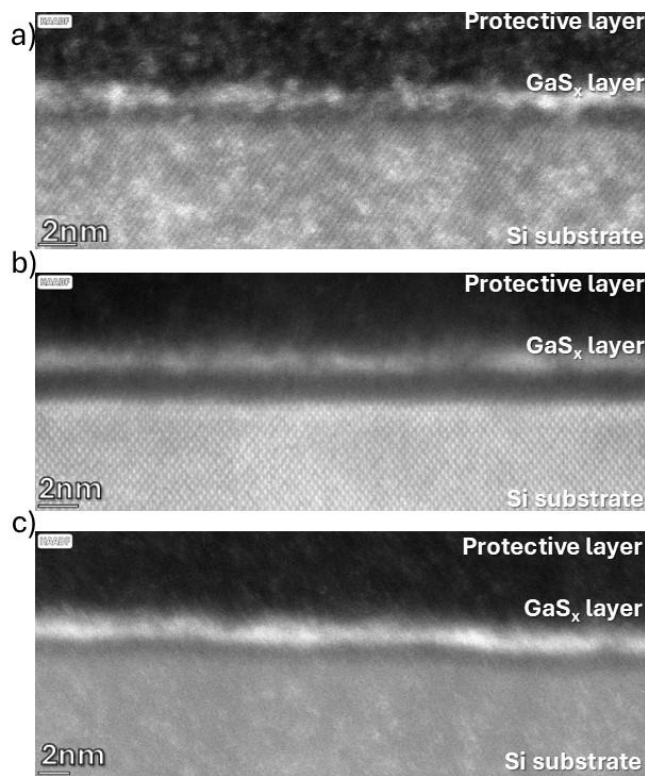


Fig. 7. TEM micrographs of the nucleated islands a) after 5 ALD cycles on an untreated surface, b) after 15 cycles on an untreated native oxide surface, and c) after 20 cycles on a DMDS treated surface

TEM microscopic analysis of the surfaces also corroborated the above results. The untreated surface, after 5 ALD cycles, clearly exhibited islands on the surface. After 15 cycles, the islands cover most of the surface. The DMDS treated surface after 20 ALD cycles has a continuous layer of GaS_x material, with a thickness of 1,5 nm.

Puurunen et al. [29,30] described the island-like growth characteristic of ALD processes and the subsequent coalescence of the islands, which depend on the surface properties and precursor chemistry. They also developed a mathematical framework that relates the growth per cycle (GPC) to fundamental physical and chemical parameters presenting a phenomenological growth model based on the following assumptions:

- Nucleation initiates exclusively on active defect sites of the substrate
- The active defect regions expand during growth, while no new nucleation sites are generated.
- The islands grow laterally and symmetrically from the nucleation centres.

The model employs basic material constants of the deposited compound and four independent parameters: the growth rate on the activated substrate, the growth rate on the already deposited ALD material, the number of cycles required for island coalescence (n_c), and the initial radius of the active areas (r_0). From these parameters the model predicts surface coverage, growth per cycle and the total amount of deposited material as functions of cycle number. Conversely, by fitting the experimentally determined surface coverage (from AFM and XPS depth information) as a function of cycle number to the model, the initial chemical quality of the substrate may be inferred. In particular, the characteristic size of the nucleation sites, their density and spatial



distribution, and the effective activity of anchoring sites can be extracted, thereby quantifying how different chemical pretreatments modify the surface and alter nucleation kinetics.

The model was implemented in Python, and the independent parameters were optimised by fitting to the measured surface coverage data. The GPC on the ALD-grown material was estimated from experiment, assuming that the deposited film possessed bulk stoichiometry and density. Surface coverage values derived from AFM measurements were used as input data for the parameter optimization. The parameters obtained from the fitting based on the phenomenological growth model are summarised in the last two rows of Table 1., where R_0 is the radius of the initial active defect sites, and represents the average spacing between the initial active defect areas. The results indicate that the original nucleation sites are not point-like. R_0 distance is the distance between the original defect sites, and n_c is the number of cycles required for coalescence, which are in good agreement with the experiments.

Coverage/subs	Si	Si+piranha	DMDS	DTBDS	piranha+DMDS
5 cycles	26	58	71	53	74
10 cycles	47	83	87	79	96
15 cycles	63	92	91	92	100
20 cycles	73	95	97	95	100
R_0	7 nm	4 nm	6 nm		2 nm
R_0 distance	16 nm	10 nm	13 nm		13 nm
n_c	26	16	16		6

Table 1. Surface coverages and calculated initial defect site sizes and distribution

IV. Conclusions

GaS was deposited with a combination of Hexakis(dimethylamido)digallium and H₂S. The experiments demonstrated that nucleation of GaS on Si is strongly dependent on the initial surface chemistry. Hydroxylated surfaces favour island-like, discontinuous growth, while thiolated surfaces—particularly those modified by DMDS—promote higher nucleation density and faster coalescence of the growing

film. These findings provide a practical pathway to improving the quality of GaS layers deposited by ALD and highlight the potential of gas-phase thiolation treatments for other sulfide systems as well. The experimental observations support the conclusion that direct sulphur functionalisation—particularly when achieved through compact disulphide molecules such as DMDS—provides a surface chemistry that is both chemically and structurally conducive to uniform GaS nucleation.

The surface functionalisation strategy developed in this work represents a notable innovation in the atomic layer deposition of metal sulfide thin films. By converting surface hydroxyl groups into sulfur-containing species, the nucleation of GaS_x was accelerated, producing uniform and nearly continuous layers at low cycle numbers. This approach demonstrates that surface chemistry can be engineered at the molecular level to overcome intrinsic nucleation barriers in sulfide ALD. The method provides a broadly applicable framework for metal sulfide systems, showing that chemically specific surface functionalisation may be a strategy for improving nucleation.

Acknowledgement

The work was supported by the project: VEKOP-2.3.2-16-2016-00011, while the microscope facility invested from project VEKOP-2.3.3-15-2016-00002 was utilized. The authors also wish to thank the Ministry of Innovation and Technology of Hungary from the National Research, Development and Innovation Fund, financed under the TKP2021 funding scheme, grant number TKP2021-NVA-03, the Hungarian National Science Fund OTKA (Grant No. FK139075).

Author declarations

Conflicts of interest

The authors have no conflicts to disclose.

Data Availability Statement:

The datasets generated and analysed during the current study are available from the corresponding author upon reasonable request. This includes AFM raw images and height profiles, XPS spectra, UV–vis absorbance data, Tauc plot calculations, SEM, and TEM images of the GaS_x films. Derived data supporting the findings of this study are also included within the article and its figures.

References

- ¹R. L. Puurunen, *J. Appl. Phys.* 97, 121301 (2005).
- ²P. Sundberg, M. Karppinen, *Beilstein J. Nanotechnol.* 5, 1104 (2014).
- ³A. A. Bol et al., *NEVAC Blad* 58, 36 (2020).
- ⁴A. Devi, *Coord. Chem. Rev.* 257, 3332 (2013).
- ⁵V. Cremers, R. L. Puurunen, and J. Dendooven, *Appl. Phys. Rev.* 6, 021302 (2019).
- ⁶M. Chhowalla, H. S. Shin, G. Eda, L.J. Li, K.P. Loh, H. Zhang, *Nat. Chem.* 5, 263 (2013).
- ⁷J. R. Bakke, J.S. King, H.J. Jung, R. Sinclair, S. Bent, *Thin Solid Films* 518, 5400 (2010).
- ⁸D. Voiry, A. Mohite, and M. Chhowalla, *Chem. Soc. Rev.* 44, 2702 (2015).
- ⁹M. A. Lukowski, A.S. Daniel, F. Meng, A. Forticaux, L. Li, S. Jin *J. Am. Chem. Soc.* 135, 10274 (2013).
- ¹⁰A. Sharma et al., *ACS Mater. Lett.* 2, 1532 (2020).
- ¹¹T. F. Jaramillo, K.P. Jorgensen, J. Bonde, J.H. Nielsen, S. Horch, I. Chorkendorff, *Science* 317, 100 (2007).
- ¹²H. Zhang, L.-M. Liu, and W.-M. Lau, *J. Mater. Chem. A* 1, 10821 (2013).
- ¹³A. M. van der Zande, P.Y. Huang, D.A. Chenet, T.C. Berkelbach, Y. You, G.H. Lee, T.F. Heinz, D.R. Reichman, D.A. Muller, J.C. Hone, *Nat. Mater.* 12, 554 (2013).
- ¹⁴K. Kang, S. Xie, L. Huang, Y. Han, P. Y. Huang, K. F. Mak, C.J. Kim, D. Muller, J. Park, *Nature* 520, 656 (2015).

- ¹⁵A. AlMutairi, Controlled fabrication of native ultra-thin amorphous gallium oxide from 2D gallium sulfide for emerging electronic applications, arXiv (2024).
- ¹⁶G. Micocci, R. Rella, and A. Tepore, *Thin Solid Films* 172, 179 (1989).
- ¹⁷P. Sastry and D. P. Dutta, *J. Alloys Compd.* 487, 351 (2009).
- ¹⁸X. Meng, J. A. Libera, T. T. Fister, H. Zhou, J. K. Hedlund, P. Fenter, and J. W. Elam, *Chem. Mater.* 26, 1029 (2014).
- ¹⁹J. Kuhs, Z. Hens, and C. Detavernier, *J. Vac. Sci. Technol. A* 37, 020915 (2019).
- ²⁰F. Mathew, N. Poonkottii, E. Solano, D. Poelman, Z. Hens, C. Detavernier, and J. Dendooven, *J. Vac. Sci. Technol. A* 41, 060401 (2023).
- ²¹N. Schneider, M. Frégnaux, M. Bouttemy, F. Donsanti, A. Etchéberry, and D. Lincot, *Mater. Today Chem.* 10, 166 (2018).
- ²²R. Zhao and X. Wang, *Chem. Mater.* 31, 445 (2019).
- ²³T. Haukka and T. Suntola, *Interface Sci.* 5, 119 (1997).
- ²⁴Z. Baji, Z. Labadi, Z. E. Horváth, G. Molnár, J. Volk, I. Bársony, and P. Barna, *Cryst. Growth Des.* 12, 5615 (2012).
- ²⁵Z. Baji, Z. Fogarassy, O. Hakkel, and Z. Szabó, *J. Vac. Sci. Technol. A* 43, 2 (2025).
- ²⁶M. Ylilammi, *Thin Solid Films* 279, 124 (1996).
- ²⁷R. L. Puurunen and W. Vandervorst, *J. Appl. Phys.* 96, 7686 (2004).
- ²⁸R. L. Puurunen, *Chem. Vap. Depos.* 9, 249 (2003).
- ²⁹M. A. Alam and M. L. Green, *J. Appl. Phys.* 94, 3403 (2003).
- ³⁰G. Parsons, *J. Vac. Sci. Technol. A* 37, 020911 (2019).
- ³¹E. Finocchio, E. Macis, R. Raiteri, and G. Busca, *Langmuir* 23, 5 (2007).
- ³²H. Li, R. Zhao, J. Zhu, Z. Guo, W. Xiong, and X. Wang, *Chem. Mater.* 32, 8885 (2020).
- ³³Z. Jin, S. Shin, D. H. Kwon, S. Han, and Y. Min, *Nanoscale* 6, 14453 (2014).
- ³⁴S. J. A. Zaidi, M. A. Basit, and T. J. Park, *Chem. Mater.* 34, 7106 (2022).



This is the author's peer reviewed, accepted manuscript. However, the online version of record will be different from this version once it has been copyedited and typeset.
PLEASE CITE THIS ARTICLE AS DOI: 10.1116/6.0005254

³⁵N. P. Dasgupta, X. Meng, J. W. Elam, and A. B. F. Martinson, *Acc. Chem. Res.* 48, 341 (2015).